Adsorption of Methyl Ester Sulfonate at the Air–Water Interface: Can Limitations in the Application of the Gibbs Equation be Overcome by "Computer Purification"?

Hui Xu,[†] Peixun Li,[‡] Kun Ma,[‡] Rebecca J. L. Welbourn,[‡] Jeffrey Penfold,[‡,‖]
David W. Roberts,[¶] Robert K.Thomas,[*,§] and Jordan T. Petkov[†,⊥]

†KLK Oleo, SDN BHD, Menara KLK, Muliara Damansara, 47810, Petaling, Jaya Selanger, Malaysia

‡Rutherford-Appleton Laboratory, Chilton, Didcot, Oxon, OX11 0QX, United Kingdom

¶Liverpool John Moores University, Liverpool, UK

§Physical and Theoretical Chemistry Laboratory, South Parks Road, Oxford, OX1 3QZ, United Kingdom

‖Physical and Theoretical Chemistry Laboratory, South Parks Road, Oxford, OX1 3QZ, United Kingdom

⊥Current address: Lonza UK, GB-Blackley, Manchester, Lancs., M9 8ES, United Kingdom

E-mail: robert.thomas@chem.ox.ac.uk

Abstract

We describe a new laboratory synthesis of the α–methyl ester sulfonates, based on direct sulfonation of the methyl ester by SO_3 introduced from the vapour phase. This was used to synthesize a chain deuterated sample of αC_{14}MES, which was then used to measure the surface excess of αC_{14}MES directly at the air/water interface over a wide range of concentration using neutron reflection. The adsorption isotherm could be fitted to an empirical equation close to a Langmuir isotherm and gave a limiting surface excess of $3.4 \pm 0.1 \times 10^{-6}$ mol m^{-2} in the absence of added electrolyte. The neutron measured surface excesses were combined with the integrated Gibbs equation to fit the variation of surface tension with concentration ($\sigma - \ln C$ curve). The fit was exact provided that we used a prefactor consistent with the counterion at the surface being an impurity divalent ion, as has previously been found for sodium diethylhexylsulfosuccinate (Aerosol OT or AOT) and various perfluorooctanoates. The critical micelle concentration (CMC) was determined from this fit to be 2.4 ± 0.3 mM in the absence of electrolyte. In the presence of 100 mM NaCl this contamination was suppressed and the $\sigma - \ln C$ curve could be fitted using the integrated Gibbs equation with the expected prefactor of 1. The new data were used to reinterpret measurements by Danov et al. on an unpurified sample of αC_{14}MES for which a computer refinement was used to try and eliminate the effects of the impurities.

Introduction

The α–methyl ester sulfonates (MES, Figure 1) are anionic surfactants prepared from renewable resources and are attractive substitutes for their petroleum derived counterparts (see e.g. Martinez et al.[1,2]). Their surface characterization has been hampered in part by the difficulty of laboratory based syntheses. For example, there is not yet an experimental determination of the limiting surface excess, Γ_{CMC}, adsorbed at the air–water interface at the critical micelle concentration (CMC) using anything other than industrial samples. Apart from a number of known impurities at significant levels, industrial samples are not usually monodisperse in chainlength. Thus, Patil et al. recrystallized a sample of C_{16}MES from the Malaysian Palm Oil Board (MPOB) and used surface tension (ST) and the Gibbs equation to obtain a value of $\Gamma_{CMC} = 1.23 \times 10^{-6}$ mol m^{-2},[3] which is obviously anomalously low. Wong et al. also recrystallized a sample from the MPOB before use and their ST data similarly suggest an anomalously low value of Γ_{CMC}.[4] Given that both these authors' measurements of the CMC are otherwise in reasonable agreement with other measurements, including ones based on lab synthesized samples,[5–7] the shallow slopes of their ST plots suggest either problems in the application of the Gibbs equation to their ST data and/or serious contamination by impurities. Danov et al. have recently adopted an approach which in principle avoids the difficulty of applying the Gibbs equation to an impure system and which they call "computer purification".[8] Their samples were also industrial samples from the MPOB but, unlike Patil et al. and Wong et al. they did no purification of their own. They measured the ST of C_nMES with $n = 12, 14, 16, 18$ in electrolyte, but not in the absence of electrolyte, and combined these results with conductivity measurements to obtain adsorption isotherms. In their words "the purification can be carried out by computer fits of an appropriate set of data from conductivity and surface-tension measurements.....In this way, one can obtain, e.g., the ST of the purified surfactant, which otherwise would demand considerable experimental efforts." Since it is relatively easy to do the recrystallizations needed to give some added purity to the industrially prepared MES, it seems that Danov et al. deliberately chose to work with an unpurified sample in order to test the idea that "computer purification" in such situations is feasible. This is an interesting idea and would be exceedingly useful if it worked, but it needs to be tested. The overall result is that there is still no determination of Γ_{CMC} on a non-industrial sample. The purpose of the present work was to make an accurate determination of Γ_{CMC} for the most commonly used MES, C_{14}MES.

We have shown previously that failures of the Gibbs equation to give correct surface excesses from ST measurements are quite common, particularly for anionic surfactants.[9]

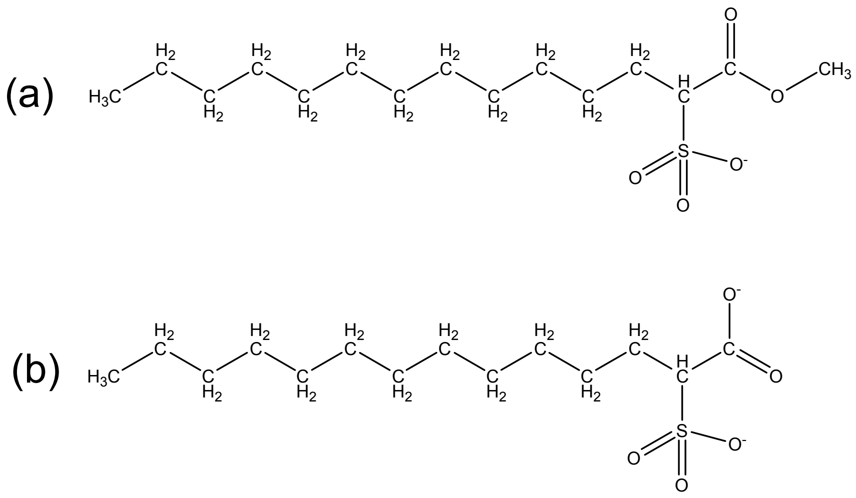

Figure 1: Structures of the surfactant ions of (a) C_{14}MES and (b) its main impurity, the di-anion where there is no methyl on the carboxy group.

The Gibbs equation is a rigorous thermodynamic equation (see Radke for a recent review[10]) and must hold for equilibrium at the air–water interface. Its "failures" for anionic surfactants are mostly failures of experimenters to identify correctly the counterion, or other species, adsorbing at the surface. This knowledge is essential for the correct application of the equation but it is not usually available. For example, contamination was shown explicitly by Cross and Jayson who used radiotracers to identify the presence of Ca^{2+} in adsorbed sodium dodecyl sulfate (SDS).[11] Contamination at a low level by Ca^{2+} ions leads to a Gibbs prefactor of 3 for the divalent surfactant salt with an approximately halved surfactant ion coverage because there are two surfactant ions in the divalent salt. The nett result is that the apparent Gibbs prefactor is approximately 3/2 instead of the expected value of 2, and this leads to a substantial underestimate of the coverage.[12] This is likely to be the cause of the low results for Γ_{CMC} obtained by Wong et al. and Patil et al. Neutron reflection (NR) allows the direct measurement of the excess of the surfactant ion without assumptions about the nature of the counterion and this can be used to test whether or not the Gibbs equation is being applied correctly. Examples where contamination by divalent counterions is particularly are the perfluorooctanoates[12] and sodium diethylhexylsulfosuccinate (Aerosol

OT or AOT).[13,14]

NR requires deuterium labelled surfactant, which means that it requires a laboratory based small scale synthesis. Although Stirton et al. described a two step laboratory synthesis,[5,15] the costs of preparing isotopic material are high and can be significantly reduced by using a single step reaction, such as used in the industrial method. The industrial method has one further potential advantage over the original lab synthesis in that it avoids the introduction of Ba^{2+} ions into the system, which is a potential source of residual divalent ions and the associated problems with the Gibbs equation described above. We have therefore devised an alternative laboratory synthesis, modelled on the industrial synthesis, but eliminating some of the less desirable features such as the bleaching step.

Experimental Details

Method of Synthesis

Following the industrial synthesis of the alkyl methyl ester sulfonate we used the direct sulfonation of the methyl ester by SO_3 introduced through the vapour phase. The methyl ester, typically 25 g, to which 2-5% by weight of anhydrous sodium sulfate had been added, was held at 80 ^oC and stirred with a magnetic stirrer under a reflux condenser. The SO_3 vapour was generated by dripping liquid SO_3 (Sigma–Aldrich or distilled from oleum) into an empty hot flask held at a temperature not greater than 100 ^oC and sweeping it over into the stirred methyl ester with dry nitrogen. The flow was adjusted to prevent too high a rise of temperature in the exothermic reaction. Almost all the SO_3 was found to be absorbed by the ester. Any residual SO_3 exiting from the reaction vessel was absorbed by reaction into an alkyl benzene of low volatility. The total amount of SO_3 passed into the system was 1.3 x moles of the starting methyl ester.

When the SO_3 had all been added the ester reaction vessel was held at 80 ^oC for another 45 min (the "resting period", in which the rapidly formed intermediate reaction products with 2:1 SO_3/ester stoichiometry slowly convert to MES and also sulfonate the remaining

ME to give MES[16]). At the end of this period a "re-esterification" step was carried out in which methanol (0.3 x moles of ester) was added as follows. The outlet at the top of the condenser was removed and methanol poured in at a rate so that methanol condensation did not rise above about half way up the condenser. This occurs because the methanol reacts exothermically and the temperature of the reaction is already at about the boiling point of methanol. The re-esterification step minimizes the production of the undesirable diacid. Crude, but not highly coloured, MES was extracted from the sulphonated and re-esterified reaction mixture, now a very dark coloured and highly viscous semi-solid, by trituration (three times) with boiling petroleum ether (80-100^{o}C). The cloudy petroleum ether solution was decanted leaving a crude dark coloured tar behind, which was retained for further extractions. Evaporation of the petroleum ether from the three extractions gave the crude MES in acid form.

Neutralization was as follows. The sample was placed in a 250 ml flask and with the temperature controlled at 30 ^{o}C, 20% aqueous Na_2CO_3 was used to neutralize the solution to pH 7–9, which led to precipitation of the MES. The crude MES in aqueous solution was treated with charcoal two or three times to remove discoloration. The product was then freeze dried and recrystallized three times from water at 4 ^{o}C before two final recrystallizations from ethanol.

The normal fully protonated and the fatty acid chain perdeuterated samples were made on the same scale and in the same way. The deuterated methyl ester, $C_{12}D_{26}CD(SO_3)C)_2CH_3$ was prepared using standard methods from perdeuterated $C_{13}D_{27}COOH$ and non-deuterated methanol. The purity of the product and the level of deuteration of the initial fatty acid was determined by proton and deuterium NMR. The deuteration level was 98% and this was maintained in the final product, including the deuterium in the α position. It is important to note that the level of purity required for an accurate determination of Γ_{CMC} using ST and the Gibbs equation is higher than can be assessed with conventional analytical techniques. NR is much less vulnerable to impurity.

Finally, we note that SO_3 is difficult and dangerous to handle because of its exceptionally high reactivity. Gloves and full face protection should always be worn. A large evaporating dish full of anhydrous sodium carbonate (soda ash) should be at hand to scatter on any spillages and vessels of liquid SO_3 should stand in it or be surrounded by kieselguhr. Small quantities can be disposed of by pouring onto a large excess of soda ash in a fume hood. Disposal of larger quantities is best done by vaporizing it into a low volatility alkyl benzene or a methyl ester of a long chain alkanoic acid.

Surface Measurements

The ST measurements were performed on a Krüss K10T digital tensiometer using a platinum plate and ultrapure water as reference. The temperature was controlled at $298 \pm 0.1K$ by a Haake K15 water bath. The solutions were contained in a glass vessel (48 mm diameter and 30 mm depth) and kept in the instrument for 10 min. before the surface tension was measured. The most concentrated solution was measured first and subsequent concentrations were obtained by dilution. The average of three consecutive surface tension measurements was taken and the plate was washed in ultrapure water and flame dried immediately before each measurement.

The NR measurements were made on the INTER reflectometer at ISIS[17] using a fixed glancing angle of incidence $\theta = 2.3^o$ and a range of wavelengths, λ, sorted by time of flight, to measure the reflectivity (R) as a function of momentum transfer vector, Q ($Q = 4\pi(\sin\theta)/\lambda$). The Q range was $0.03 - 0.3$ Å^{-1}. The reflected intensity was normalised to the direct beam and the absolute reflectivity values were calibrated by reference to the reflectivity from the surface of D_2O, for which the Q range was extended to include the critical edge for total reflection. The samples were contained in sealed Teflon troughs held at $298K$ and containing a sample volume of $\approx$ 25 mL Each individual NR measurement took 15 to 30 minutes and the measurements were made in sequence in a 7 position sample changer. The Teflon troughs were cleaned in between measurements with ultrapure water and ethanol.

All the measurements used null reflecting water (NRW), in which the isotopic composition (H/D) had been adjusted to make its neutron refractive index exactly the same as that of air. There is then no reflected signal in the absence of adsorbed species. The background scattering, from incoherent scattering and multiple diffraction from the bulk liquid, is at a level of about 2×10^{-6} relative to 100% reflection (see Figure 2). This does not vary with Q and is typically 2-3 orders of magnitude lower than the reflection from a deuterated surfactant layer, i.e. it is easy either to subtract or to incorporate in the fitting process. When the solvent is NRW, the reflectivity is given by

$$R = \frac{16\pi^2}{Q^4} \left|\hat{\rho}'(Q)\right|^2 \tag{1}$$

where $\hat{\rho}'(Q)$ is the 1 dimensional Fourier transform of the gradient of the scattering length density profile normal to the interface. If the aim of the experiment is to measure just the surface coverage of surfactant, this can be reduced to the simpler equation

$$R(Q) = \frac{64\pi^2}{Q^4} \rho^2 sin^2 \left(\frac{Qd}{2}\right) \tag{2}$$

where d and ρ are the thickness and scattering length density of the adsorbed layer. For a single surfactant species at the interface the surface excess, Γ, is given by

$$\Gamma = \frac{d\rho}{N_a \sum b} \tag{3}$$

where $\sum b$ is the sum of the neutron scattering lengths of the nuclei comprising the surfactant. This sum can be calculated from the isotopic composition and stoichiometric formula of the surfactant and the known scattering lengths of the isotopic species. The value of the product $d\rho$, and therefore of the surface excess, is independent of the structural model used for the surface layer over most of the Q range used for these experiments. This is not the case for the individual values of d and ρ.

Results

A selection of neutron reflectivity profiles for C_{14}MES containing a $C_{13}D_{26}$ fragment are shown in Figure 2(a) and the surface excesses of the surfactant ion for the whole set of concentrations are shown in Figure 2(b). For the purposes of using the integrated Gibbs equation it is necessary to have a parameterized functional form for the adsorption. We found that the data in Figure 2(b) come close to fitting a Langmuir isotherm but the fit is not accurate enough for the integration. However, a fit of the inverted form of the isotherm to a polynomial results in the fit shown in the Figure. There is no significance to this form, the only important feature being that it is a satisfactory fit of a single function to the whole set of data. It is nevertheless not far from a Langmuir isotherm. Taking the average of the six highest concentration measurements leads to a mean saturation coverage of $3.4 \pm 0.1 \times 10^{-6}$ mol m^{-2}. As discussed previously,[9,18] NR is affected by deuterated impurities but in a very different way to ST. Both ST and NR are most noticeably affected in the vicinity of the CMC. If the impurity derives from a product related to the deuterated surfactant, NR may overestimate the adsorption until the concentration is high enough that the impurity is dissolved in the micelles, i.e. at a concentration slightly above the CMC. It can be seen that there is a slightly anomalous high point in Figure 2(b) at a concentration of 2.9 mM. Since most such anomalies have been observed, in practice, immediately above the CMC,[9] this suggests that the CMC is probably slightly below this concentration, but it should be emphasized that there is no clear criterion for deducing a CMC from the neutron isotherm, as has been fully discussed elsewhere.[9] In addition to the set of measurements fitted in Figure 2(b) we obtained a value of the coverage of 3.56×10^{-6} mol m^{-2} in the presence of 100 mM NaCl at 5 mM C_{14}MES, a slight increase from its limiting value in the absence of electrolyte. Finally we made the important measurement of a 50:50 mixture of protonated and deuterated forms and obtained a surface excess identical with that for the fully deuterated compound at 6 mM. This test is important because it confirms that (a) there is no isotope effect on the adsorption, and (b) that the level of purity is not only

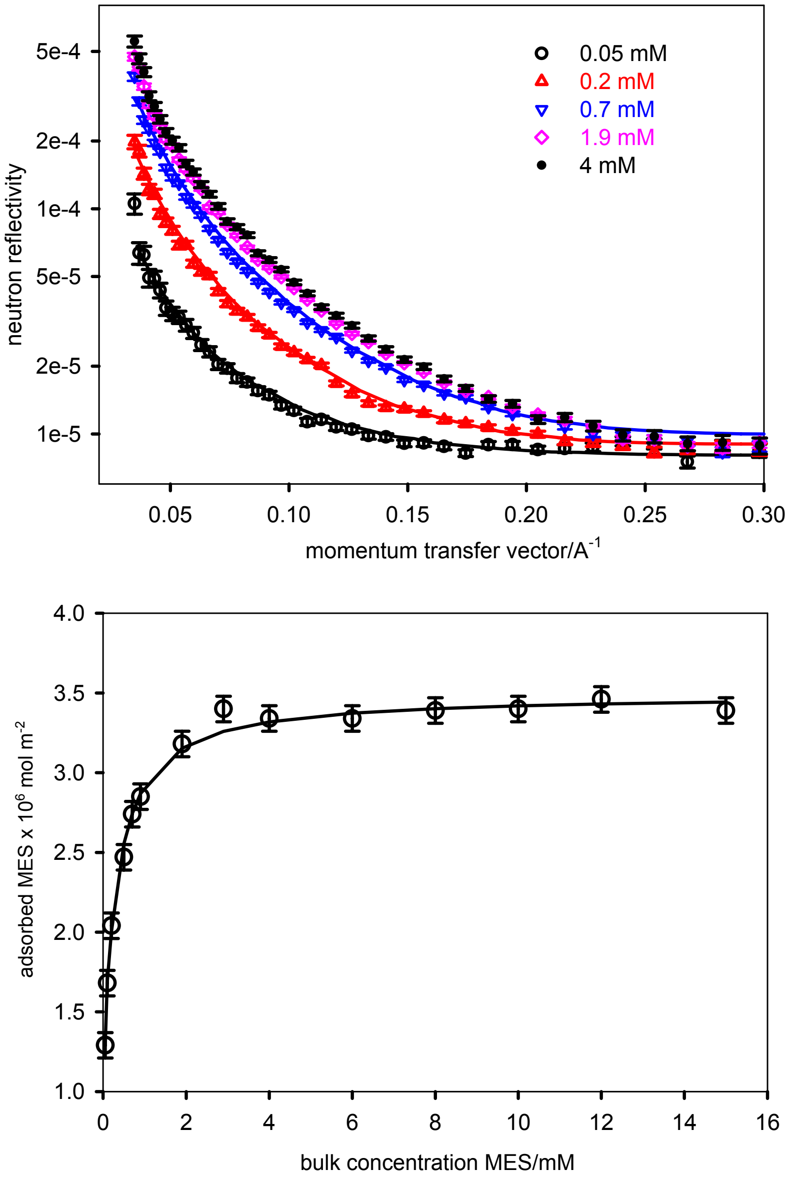

Figure 2: (a) Neutron reflectivity profiles of chain deuterated C_{14}MES obtained at different concentrations. The reflectivity is on a log scale and the surface excess is directly proportional to the square root of the reflectivity at the lowest value of the momentum transfer vector. (b) The complete set of values of the measured surface excess fitted to a polynomial based on the inverted Langmuir isotherm.

comparable but is probably high in both protonated and deuterated samples.

There are no published ST data for C_{14}MES on its own without added electrolyte. Danov et al. have given the results of measurements with 10 mM NaOH added and with the further addition of 20 and 100 mM NaCl. Their reason for adding NaOH was to neutralize unspecified acidic species and we discuss this further below. Unless the addition of NaOH causes precipitation its addition is equivalent to adding 10 mM of a sodium salt, i.e. the prefactor in the Gibbs equation should be 1. Their ST measurements therefore measure the CMC and the surface excess of surfactant only in the presence of a sodium electrolyte, in which the excess Na^+ should suppress any anomaly resulting from contamination by other ions. Our ST results for the surfactant on its own are shown in Figure 3(a). The CMC and limiting surface tension at the CMC in 100 mM NaCl are shown in Figure 3(b). In the measurement in the absence of salt there is a small minimum in our ST curve indicating the presence of an impurity, which we discuss further below.

The fitted adsorption isotherm from the NR data can be used with the integrated Gibbs equation to calculate the ST curve below the CMC in the absence of added NaCl. If it is assumed that the adsorbed counterion is entirely Na^+ the Gibbs prefactor is 2, but if the counterion in the surface layer is M^{2+} as a result of a low level of contamination of the original sample by divalent ions, the Gibbs prefactor would be approximately 3/2. This is a combination of a Gibbs prefactor of 3 and an approximately halved surfactant ion coverage caused by the presence of two chains in the divalent salt. The calculated curves for both 3/2 and 2 are shown in Figure 3 and it is clear that the correct curve, which fits the ST extremely well, is 3/2, i.e. the sample appears to be contaminated by divalent ions. That this is only a surface contamination is shown by the value of the CMC, which is significantly higher than that for the calcium surfactant (0.66 mM[19]). This excellent fit of the integrated Gibbs equation to the data in the absence of added electrolyte gives a value of the CMC of 2.4 ± 0.3 mM, slightly lower than the average of 2.8 ± 0.3 mM from the 3 values from Stirton et al., Fujiwara et al., and Wong et al., and much lower than the value of 3.98 mM given by

Danov et al.

The behaviour of the ST for C_{14}MES without added NaCl is similar to that previously identified in various monovalent salts of fluorocarbon carboxylates and in AOT related surfactants. A further similarity suggestive of contamination by unspecified multivalent ions is that when we attempted to purify a sample of C_{14}MES on a silica column, the product had an anomalously low CMC at 1.3 mM. This is intermediate between the value of 2.4 mM for the pure compound and the value for pure calcium C_{14}MES of 0.66 mM. This difference can only result from an incomplete replacement of Na^+ by Ca^{2+} or by a more complicated ion mixture from the high area silica used for the column. The same effect was found when we tried to purify AOT on a column.[13] In previous papers we showed that traces of divalent ions from AOT solutions could be removed by the addition of low concentrations of the Ca^{2+} sequestering agent tetrasodium ethylene diamine tetra–acetate (EDTA) and the same method has been adopted by Eastoe et al.[14,20] Thus addition of EDTA changed the apparent Gibbs prefactor for AOT from 3/2 to the expected value of 2. However, the addition of EDTA at similar levels to those used for AOT failed to correct the anomalous slope of the ST curve for C_{14}MES. The level of EDTA that can be added must be at a low enough concentration that it does not introduce ionic strength effects. Its efficacy at this low concentration of typically less than 1 mM then depends on the level of impurity of the divalent ion, which is not known, and on the balance of the binding constants of the divalent ions between the EDTA and the surfactant ion in question, the last of which is also not known.

We have speculated previously that the evidently strong binding of a divalent M^{2+} to AOT has a contribution from the chelating effect of the ester carboxy group adjacent to the sulfonate group. An AOT molecule has two possible chelating ester groups, one attached to the same carbon as the sulfonate, i.e. part of a sulfo-acetic acid grouping and the other separated by an additional CH_2 group, i.e. part of a 3-sulfo-propionic acid grouping. The C_{14}MES only has the former grouping and a possible configuration of the binding of a divalent ion to C_{14}MES at the air–water interface is shown in Figure 4 (b). In the figure

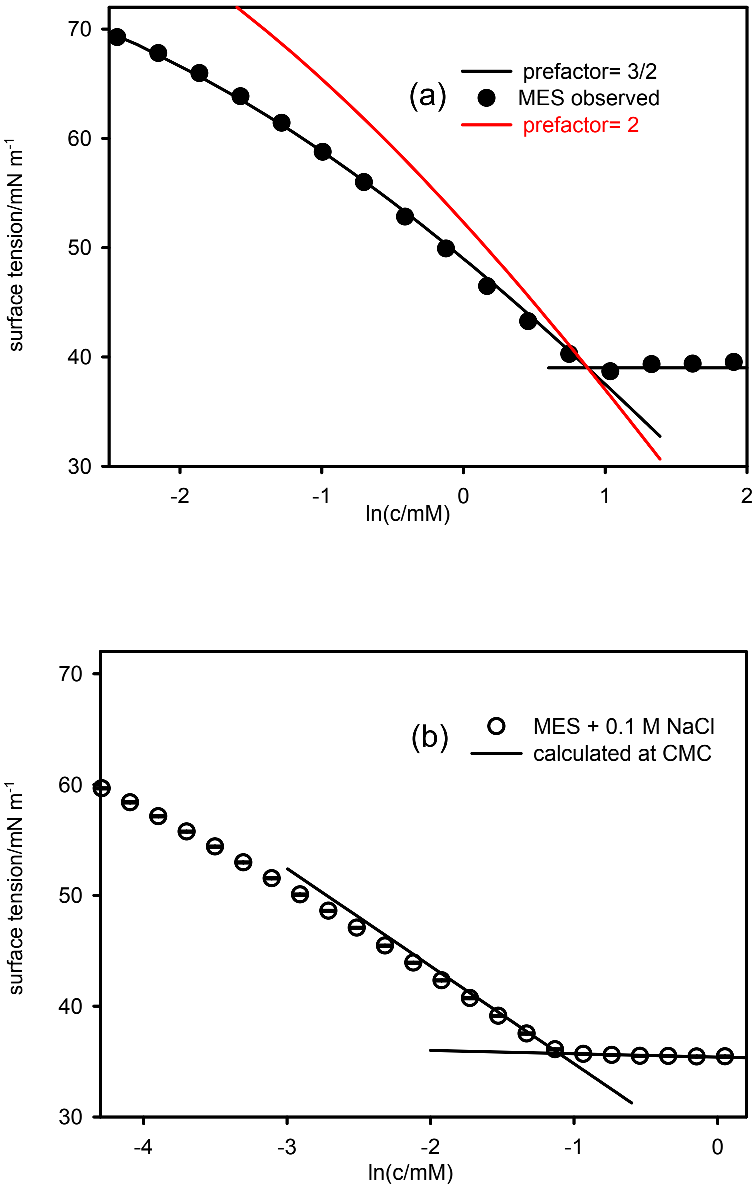

Figure 3: (a) Surface tension data for sodium C_{14}MES at 298 K with a curve calculated using the integrated Gibbs equation, the adsorption data from Figure 2, and a prefactor of 3/2 (black line) and a prefactor of 2 (red line). (b) Surface tension data for C_{14}MES at 298 K with 100 mM NaCl with a straight line, calculated using the integrated Gibbs equation, the adsorption at the CMC, and a prefactor of 1.

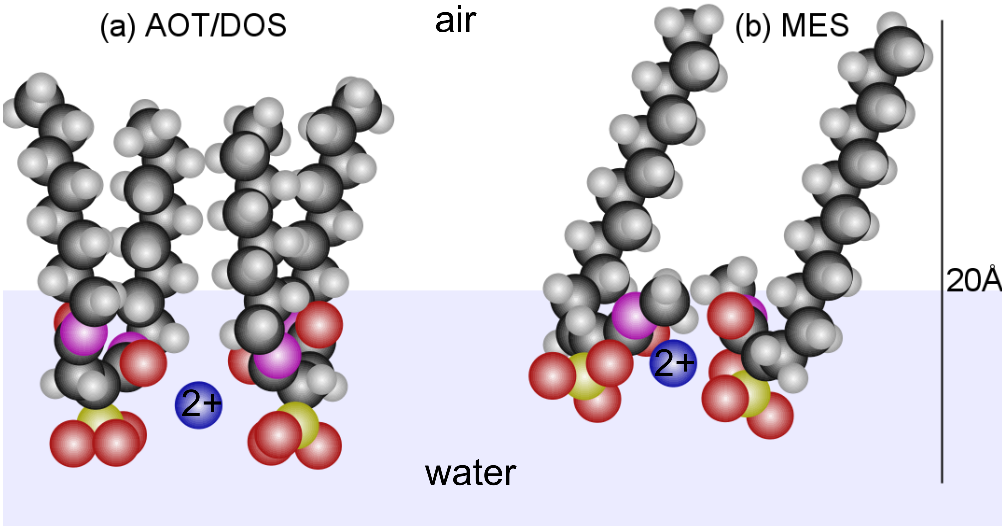

Figure 4: Possible surface arrangements of surfactant ions around a divalent cation in adsorbed layers of (a) dioctylsulfosuccinate and (b) C_{14}MES at the air water surface. The divalent ion is shown in blue, the carbonyl oxygens and the oxygens of the sulfonate in red, and the carboxy oxygens in mauve. The level of immersion in the water is typical of that estimated from NR for other surfactants, and the AOT/DOS is more immersed because the head group is more hydrophilic.

the divalent ion is in blue and the oxygen atoms are in red except for the oxygen actually forming the ester bond, which is in mauve. In the solid state the divalent ion would be expected to be sandwiched between the two singly charged sulfonate groups to form a lamellar structure. However, that cannot happen at the surface and Figure 4 (b) indicates how chelation involving the carbonyl oxygens is a likely part of the binding the divalent ion at the surface. Figure 4(a) shows the corresponding arrangement for dioctylsulfosuccinic ester. We have used the dioctyl rather than the diethylhexyl group in the illustration because the hydrocarbon tails are much simpler than in AOT itself, where there are complications with the different possible optical isomers. In DOS/AOT there is in principle a choice of carbonyl oxygen to assist the chelation. However, the sulfoacetic carbonyl group is much more spatially accessible than the propionic carbonyl. That the carbonyl of the sulfo-acetic group woulde be preferred is reinforced by the stronger acidic nature of the sulfoacetic acid grouping (the second dissociation constant, of the COOH group, for the sulfoacetic and 3-sulfo-propionic acids have pK values of 4.1 and 4.5 respectively[21]). Examination of Figure 4 suggests two reasons why the binding of a divalent ion by the chelation mechanism should be significantly stronger for the MES family of surfactants relative to the AOT family. The most important factor is that the head groups are more closely spaced in C_{14}MES than in AOT (respective area per molecule of 49 and 78 Å^2),and the second factor is that, rather than being an alternative binding arrangement, the extra carboxy ester group in the AOT family of surfactants is electron withdrawing and therefore decreases the ability of its sulfo-acetic group to chelate the divalent ion.

In the presence of 100 mM NaCl the combination of the higher surface activity (lower CMC) and the large excess of Na^+ ions should suppress the effect of divalent ion impurities and the Gibbs prefactor in the $\sigma - \ln C$ plot should be 1, i.e. the ST measurement then only determines the surface excess of the surfactant ion. Figure 3(b) shows the good agreement of the experimental ST data with the limiting integrated Gibbs equation using a prefactor of 1 and the directly observed limiting surface excess of the surfactant ion of 3.56×10^{-6} mol m^{-2} from NR. AOT and related compounds similarly behave normally in the presence of significant added NaCl.[13]

The increase in the surface excess at saturation on the addition of 100 mM NaCl is relatively small for C_{14}MES and suggests that in the absence of electrolyte counterions are already extensively bound at the surface. It is interesting to compare this behaviour with the related surfactants SDS and SLES. The CMCs of the three surfactants and the saturated surface excesses (measured above the CMC using NR) are given in Table 1. The screening effect of the added NaCl decreases strongly on changing from SDS through SLE_1S to C_{14}MES. This is consistent with the expected higher level of dissociation of SDS compared with the other two surfactants.

The main effect of the traces of ionic impurities is on the ST rather than on the NR behaviour. To test this we used NR to determine the surface excess of C_{14}MES in the presence of $CaCl_2$. At a concentration of 2 mM C_{14}MES and 0.5 mM $CaCl_2$ the surface excess was determined to be 3.65×10^{-6} mol m^{-2}, which is only about 7% higher than

Table 1: CMCs and surface excesses at saturation with and without 100 mM NaCl at 298 K. The surface excesses are all determined above the CMC using neutron reflection.[9]

surfactant	CMC/mM	$10^6 \times \Gamma$/mol m^{-2}	$10^6 \times \Gamma$/mol m^{-2} (100 mM NaCl)	% increase
SDS	8.1	3.9	4.8	23
SLE$_1$S	4.2	4.0	4.65	16
C$_{14}$MES	2.4	3.4	3.56	5

determined for the sample in the absence of electrolyte, whereas the differences in ST below the CMC are very large because of the change in CMC to 0.7 mM.

Discussion

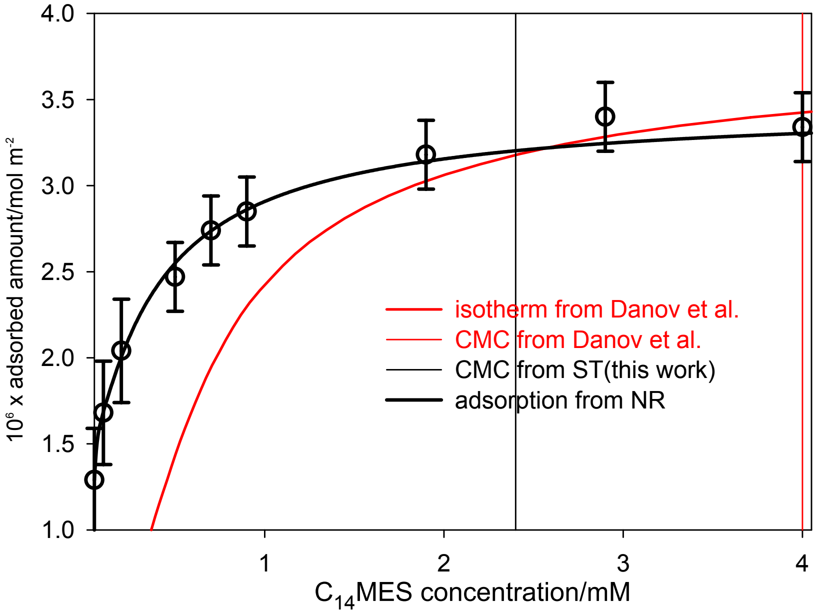

Figure 5: Comparison of the directly measured excess of C$_{14}$MES using NR at 298 K (data and fitted line as in Figure 2) with the isotherm deduced by Danov et al.[8]

Figure 5 compares the direct NR measurements of the excess of the surfactant ion with the final results of the "computer purification" (CP) analysis of Danov et al. for C$_{14}$MES.

The measured limiting coverage at high concentration from NR is slightly lower than deduced from CP. However, the main difference between the CP and NR results is in the concentration dependence of the adsorption. At first sight this might seem to be simply because of the large difference in the two CMCs, 2.4 and 3.98 mM, but the NR coverage measurements are completely independent of the value of the CMC as determined from ST. We are not able to judge the extent to which the fractional coverage calculated by Danov et al. is tied to their experimental value of the CMC, and there are therefore three possible reasons for the disagreement, (i) the NR coverage is incorrect, (ii) the CP value of 3.98 mM is too high, or (iii) the relation between adsorption and micellization required by the CP calculation of Danov et al. is not an appropriate one. The values of the CMCs of 3.98, 1.14 and 0.32 mM for C_{14}MES, C_{16}MES and C_{18}MES respectively obtained by Danov et al. are significantly higher than all previous measurements. For lab synthesized samples these previous results are 2.8, 0.4 and 0.08 mM, determined using the uv spectrum of pinacyanole chloride,[5] and 3.15, 0.73, and 0.18 mM, determined using conductivity.[6,7,19] For recrystallized industrial samples Wong et al obtained CMCs for C_{14}MES and C_{16}MES of 2.7 and 0.7 mM at 308 K[4] and Patil et al. obtained CMC values of 0.6 mM (ST) and 0.7 mM (conductivity) for C_{16}MES at 298 K.[3] This suggests that (ii) is the most probable reason for the discrepancies in Figure 5 and we therefore examine what is known about the likely impurities in the C_nMES and what effect they might have on their results.

The mechanism of the industrial sulfonation, and hence our laboratory based synthesis is relatively complex, but it has been well studied.[16] Before neutralization, the main impurities are the dianion (see Figure 1), some unreacted material and the highly coloured material. The final product usually contains the fatty acid sulfonate (disalt) as the major impurity (see e.g. Maurad et al.[22]), which has a higher Krafft temperature than the MES and makes the final product more soap-like.[23] In the laboratory synthesis, the experimental conditions are such that the coloured material is produced at a much lower level and is largely removed by solvent extraction prior to neutralization. Following neutralization any residual coloration is removed by charcoal in aqueous solution and the extensive recrystallization is expected to remove the disalt and other impurities. However, in the industrial synthesis the further reaction step of bleaching has to be carried out before neutralization and drying. The coloration is thought to arise from polysulfonated compounds with conjugated double bonds.[16,24] The chemistry of its removal by bleaching with hydrogen peroxide is not known in detail but it can be expected to add OH groups to the conjugated double bonds, which will not only remove colour but will increase water solubility, generate some new acidic species, and possibly bring about some reduction in the average carbon chain length of the impurities. This step usually precedes the final removal of residual methanol, neutralization with weak alkali, and drying. The main difference between the final industrial product and the lab product before recrystallization is that the former contains the various species produced in the bleaching stage. Given that the bleaching products are likely to be more water soluble than the MES itself, recrystallization, especially involving water, should remove most of them fairly easily. The only differences between the recrystallized industrial and lab samples may then only be that the tighter control of the reaction conditions in the laboratory should lead to less residual starting product and less of the disalt impurity.

The non-recrystallized samples of Danov et al. will therefore contain the products from the bleaching process in addition to the two main impurities of some original starting material and the disalt. An unexpected feature of these samples, as reported by Danov et al. is their marked acidity. This is shown for each of the three MES in Figure 1 of the Supporting Information of Danov et al. Just as they describe in their main paper the pH initially decreases systematically with concentration for all three samples. For the C_{12}MES and C_{14}MES this decrease in pH is from about 6 to between 4 and 5 when the CMC is reached and then there is little change above the CMC. This is characteristic of the presence of weak acids with carbon content lower than the alkanoic acid produced by hydrolysis of the starting ester, which further suggests that these species originate from the bleaching by-products. The result also shows either that neutralization of the original material was incomplete or that subsequent hydrolysis in an incompletely dry sample has led to the formation of carboxylic acid species. The starting material in either its original form or the hydrolysed form will be insoluble and highly surface active. We note in passing that the diacid is unlikely not to have been completely neutralized because the second dissociation constant (the carboxylic acid part) is likely to be high (the pK value for the related sulfo-acetic acid is 4.1[21]). There are possible by-products of the original reaction, e.g. the iso-MES (carboxylic acid anion and methylated sulfonate) and the di-MES (both groups methylated), that would hydrolyse in water to give acids but these are expected to occur at only very low levels and would, in any case, give a time-dependent pH, which does not seem to have been observed by Danov et al. Danov et al. used their measured pH to correct their conductivities for the presence of the acid species. However, for the longest chain species, C_{16}MES, the pH behaviour indicates that the acid impurities also interfere with micellization. Thus, although for the other two samples the pH decreases with concentration below the CMC, for the C_{16}MES above the CMC, the pH increases steadily back up to around the starting pH of 5.4 at about 10× CMC. This change indicates that some or all of the acid species are incorporated into the micelles and are incorporated in their *unionized* form. This would have a strong effect on the conductivity above the CMC. That no such effect was observed for C_{12}MES and C_{14}MES shows only that any acids incorporated into the micelles do not significantly change their state of ionization, it does not show that no acids are incorporated. Thus, although it is possible to correct the conductivity below the CMC for the extra pH, the corrections required above the CMC may be more complex.

For a dilute surfactant solution below the CMC, the specific conductivity, κ, is

$$\kappa = \Lambda_0 c - A c^{3/2} \tag{4}$$

where Λ_0 is the limiting molar conductivity at infinite dilution, c is the concentration, and A is a constant that takes into account the ionic interactions. In the absence of electrolyte and

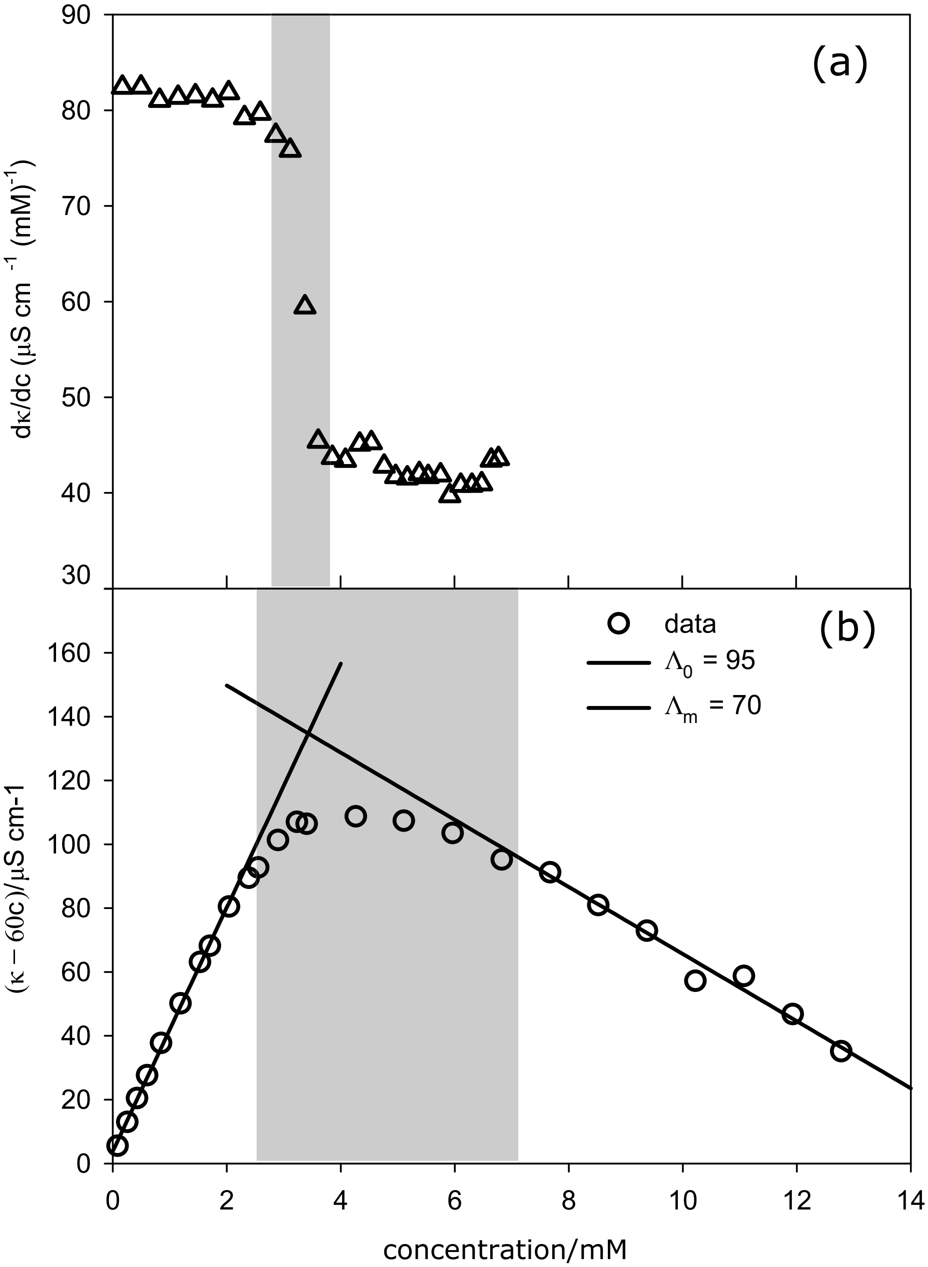

Figure 6: (a) Plot of $\delta\kappa/\delta c$ against c for C_{14}MES using data from Fujiwara[6] at 308 K. (b) Points are the conductivity, $\kappa' = \kappa - 60c$, calculated from the conductivity data of C_{14}MES solutions at 298 K after correction for pH effects from Danov et al.[8] The best fits of the two limiting straight lines shown in black intersect at 3.4 mM. In both (a) and (b) the area shaded in grey is the range of non-linear behaviour of the conductivity for the two different samples.

for the range of concentrations appropriate for C_{14}MES the second term can be neglected in the determination of the CMC. Above the CMC the specific conductivity is usually taken to be

$$\kappa_m = c_m(\Lambda_0 - \Lambda_m) + \Lambda_m c \tag{5}$$

where c_m is the intersection of the two straight line plots above and below the CMC and κ_m and Λ_m are the specific and molar conductivities above the CMC. The CMC is normally taken to be c_m and is commonly determined by fitting straight lines above and below the CMC, exactly as used by Danov et al. However, the method becomes less accurate when (i) there is extra electrolyte in the sample because this increases both slopes and hence reduces the relative difference, (ii) there is added fixed electrolyte because the second term on the right in Eqn (4) may no longer be negligible, (iii) if the conductivity of the micelles varies above the concentration of the initial micellization. In the first two cases, the sensitivity of the method is greatly improved by measuring the differential of κ (see for example, Carpena et al.[25]), when

$$\frac{\delta\kappa}{\delta c} \approx \frac{d\kappa}{dc} = \Lambda_0 - \frac{3A}{2}c^{1/2} \tag{6}$$

Thus Fujiwara et al. used a plot of the $\delta\kappa/\delta c$ against $c^{1/2}$ to determine the CMC of C_{14}MES as a function of temperature and obtained moderately sharp transitions between the plateaus of the submicellar and micellar regions. Because the CMC of C_{14}MES is low the concentration term is negligible and a simpler plot of $\delta\kappa/\delta c$ against concentration is accurate enough to pinpoint the CMC, as shown for their data at 308 K in Figure 6(a). The reason for avoiding the differential method is that it is much more time consuming, but it is clear from this plot that the method is extremely sensitive. The effect of (iii) would also be seen more clearly in the differential plot, although it then raises the question as to how the CMC should be defined.

Although the conductivity data of Danov et al. (Figure 3(b) in their paper and corrected for the pH dependency described above) seem to be well fitted by two straight lines, the difference between their slopes is not large on the scale of the data and gives little indication of any deviation from the two straight lines close to the CMC. The latter can be better examined by replotting their data in a different way. If a term Bc, where B is an arbitrary constant, is subtracted from the right hand side of Eqns (4) and (5) and we again omit the ionic interaction term, we obtain respectively

$$\kappa' = (\Lambda_0 - B)c \tag{7}$$

and

$$\kappa'_m = c_m(\Lambda_0 - \Lambda_m) + (\Lambda_m - B)c \tag{8}$$

Figure 6(b) shows the conductivity data replotted after subtracting Bc with $B = 60$ from their data. This changes the positive slope above the CMC to a negative one. It is then easy to see that the width of the non-linear region, shaded in grey, is unusually large. We have fitted two straight lines using points outside the curved region, which gives slopes of 95 and 70 (above the CMC) and an intersection at 3.4 mM, to be compared with values obtained by Danov et al. which were 89, 56 and 3.7 mM respectively. The important observation is not that this plot causes changes in the fitted values of the slopes but that it reveals an unusual width in the region of the CMC. For comparison the shaded area in Figure 6(a) shows the narrow width of the micellization in the data of Fujiwara et al.[6,26] The concentration scale is the same in the two plots. The fitted parameters for the data of Fujiwara at 298 K were respectively 70, 35 and 3.15 mM.[6,26]

Danov et al. noted that the slopes of their limiting lines were larger than would be expected for pure C_{14}MES and attributed this to the presence of an electrolyte impurity, equivalent to 14 mol% of NaCl, and most probably Na_2SO_4 on its own or with $NaMeSO_4$ (both are listed as impurities in an MPOB (the source of their samples) specification of 2006[22]). The effect of such an electrolyte would be approximately to increase the slopes of the plots above and below the CMC by a similar amount. This is consistent with their original slopes which were 89 and 56 respectively. Subtraction of 20 from each of these gives 69 and 36, in good agreement with the values of 70 and 35 obtained by Fujiwara et al. However, the agreement is less good for our re-analysis for which the subtraction of 20 would give values of 70 and 50 respectively. The higher value of Λ_m does not affect the original conclusion that there may be a contribution from an apparent simple electrolyte below the CMC but it and the large apparent width of the micellization indicates that additional, probably ionic, species have an effect on the micellization.

A mixture of two surfactants has a well defined and sharp CMC, which is clearly seen in an ST measurement. The conductivity of mixed micelles depends on the degree of dissociation per molecule for each of the surfactants, on the composition of the micelles, and on their aggregation number. Above the mixed CMC there are then several reasons why the changes in conductivity may make it difficult to determine the value of the CMC. These are (i) the component with the lower CMC preferentially fractionates into the micelles to give a micelle composition that is different from the total solution composition, and this must slowly change towards the total solution composition as the concentration increases and the micelles become the dominant species, (ii) the degree of dissociation of each surfactant will generally be different in the mixed micelle from that in the pure micelles, and this will change as a result of the changing composition, (iii) the conductivity of the micelles depends on their aggregation number and this is also likely to vary with changing composition, and (iv) all the above changes will have a secondary effect on the monomer concentration and conductivity. All these effects have been observed. Thus Mysels and Otter, using differential conductivity, found that the sharp vertical region shown in Figure 6 became very broad for several compositions in mixtures of sodium decyl and sodium dodecyl sulfates.[27] Their comment on one of their $\kappa - c$ plots was "the plot for the mixture is here too curved to make a linear extrapolation meaningful". Tokiwa and Moriyima demonstrated effects of both changes of dissociation and of aggregation number in SDS–nonionic surfactant mixtures.[28]

All of the factors in the previous paragraph may then apply over a range of concentration above the CMC until the micellar composition attains the total average composition. The consequence is that extrapolation of a straight line fit to the high concentration region, as done in Figure 6, almost certainly does not intersect the low concentration line at the CMC. The above discussion suggests that a better value would be obtained by taking the concentration where the conductivity initially deviates from the initial straight line, i.e. at about 2.2 mM, and to add the typical half-width of the micellization using the data in Figure 6(a). This gives a final value of the CMC of 2.5 mM, close to our ST result. Incorporation of this value into the CP fitting of Danov et al. would largely remove the discrepancy between the NR and CP measurements in Figure 5. The second interesting feature is that the slope of the high concentration line in Figure 6, after subtraction of the electrolyte effect is 50 compared with the value of 30 obtained by Fujiwara et al. This can only be explained by the micelles having a substantially higher conductivity than the value of 30 of Fujiwara et al. This might result from their carrying a higher charge per surfactant, or from a change in micellar size, either of which is plausible, but without more detailed information about the impurities, it is not possible to make even a semi-quantitative estimate of the effects that might occur.

Danov et al. preferred the accuracy of their value of the CMC from conductivity over that from their ST measurements. They further concluded that the lower value from the ST was a result of a nonionic impurity and made corrections in their CP for mixing on the basis of this difference. It is, however, clear from Figure 6 and their pH measurements that the conductivity measurements cannot be used to determine the CMC accurately. We therefore turn to their ST results. Given our tentative explanation of the pH behaviour, the addition of 10 mM NaOH, which was added to neutralize the acids present, has an effect on the surfactant equivalent to the addition of 10 mM of a 1:1 electrolyte. Using the integrated Gibbs equation with prefactor of 1 for a 1:1 electrolyte and our limiting coverage determined by NR for 100 mM NaCl we obtain the fits to their data shown in Figure 7(a). The observed limiting slopes are clearly consistent with the NR range of surface excess (3.4–3.56×10^{-6}

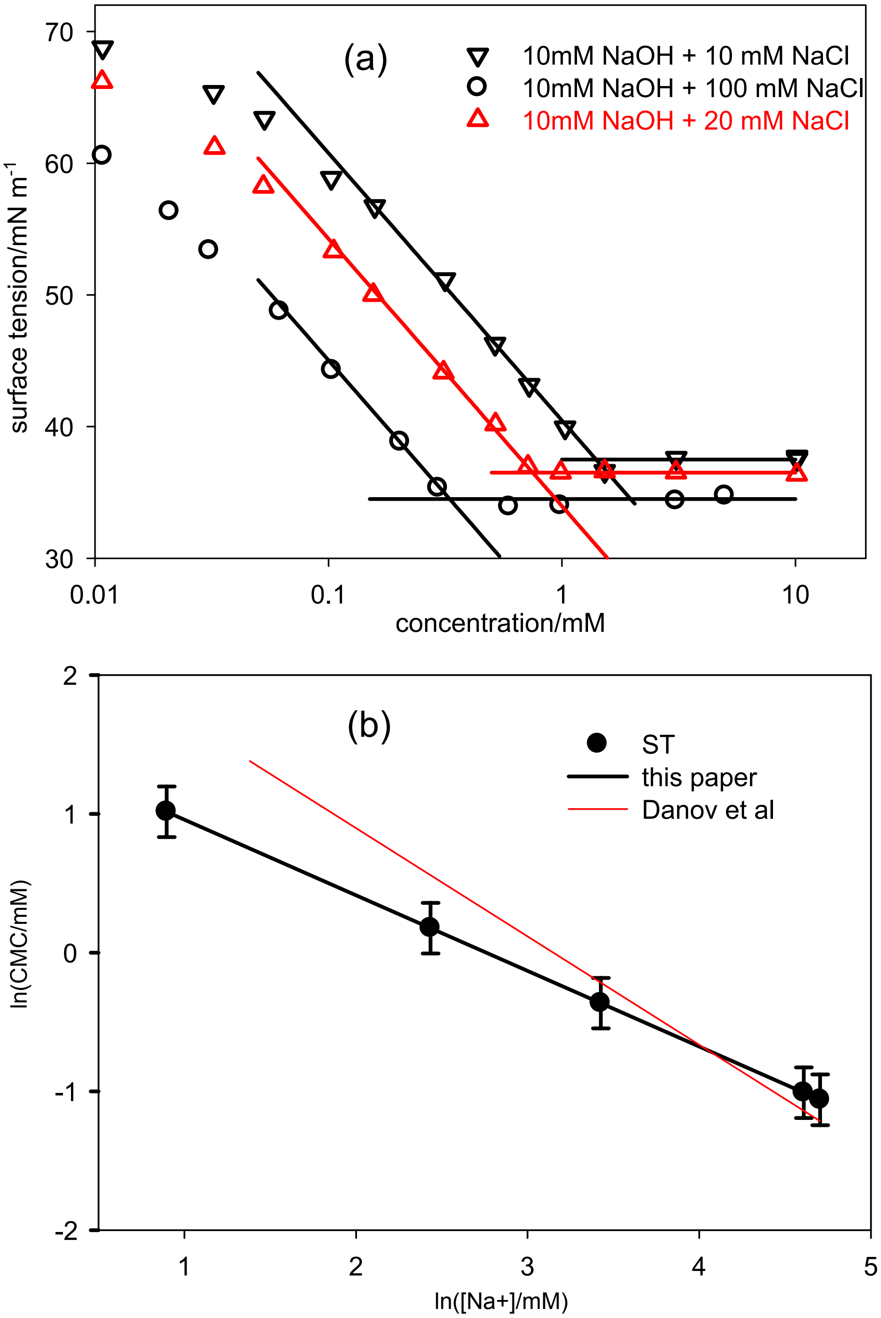

Figure 7: (a) Surface tension of solutions of C_{14}MES containing varying amounts of electrolyte. The data is from Danov et al.[8] The fitted lines below the CMC are calculated using the integrated Gibbs equation with a limiting surface excess at the CMC of 3.56×10^{-6} mol m^{-2}. (b) Corrin–Harkins plot. The black line is the best fit to the CMCs determined from ST in (a) and Figure 3. The thin red line is the equivalent plot from Danov et al. and based on the CMCs determined from conductivity measurements and "computer purification".

mol m^{-1}) and the intersections with a flat ST above the CMC give values of the CMC of 1.4 mM in 10 mM NaOH + 10 mM NaCl, 0.75 mM in 10 mM NaOH + 20 mM NaCl and 0.33 mM in 10 mM NaOH + 100 mM NaCl. These are compared with our own two values in a Corrin–Harkins plot in Figure 7(b) with the best fit of a straight line (in black). The thin red line shows the Corrin–Harkins plot obtained by Danov et al. (given in their paper as Eqn (24)), which is based on a combination of their conductivity measurements and their CP treatment. We note that their line fits exactly their three CMCs determined from the conductivity data at 0, 5 and 15 mM NaCl. The disagreement between the two analyses therefore finally comes down to the differences between the ST and conductivity results. Whether or not the ST results of Danov et al. are affected by impurity cannot be determined but their conductivity results clearly cannot be reliably used to determine the CMC.

Our value of the CMC for C$_{14}$MES is the lowest of the values so far determined. Although it is probably within the experimental error of the three other values of Stirton et al., Fujiwara et al. and Wong et al., their values are systematically larger. Since impurities generally lead to reduced CMCs the normal conclusion would be that the higher the determined value, the more reliable it is likely to be. However, the situation is somewhat different for the MES. For recrystallized samples, the main impurity is likely to be the disalt, but there may be residual amounts of the starting material. The disalt has a high limiting solubility of 36 mM.[29] Since it also has a a high Krafft temperature, the solubility is effectively equivalent to the CMC, whose high value makes it relatively surface inactive. However, it is expected to be incorporated into the C$_{14}$MES micelles and the mixed CMC will then be increased. The effect of the starting ester on the ST will be similar to that of dodecanol on SDS, i.e. it will tend to generate a minimum at the CMC which will also have the effect of apparently lowering the CMC. The presence of a small minimum in our ST data indicates that the starting material is difficult to remove completely. However, the minimum is weak and it is unlikely to cause a significant depression of the CMC. The raising of the CMC by the disalt will always be difficult to assess but, since it is the dominant impurity, a lower measured CMC is likely to be more reliable, contrary to the usual pattern of contamination. The final impurity to be considered is divalent ions. They are clearly present in our sample and probably present in the commercial samples of Wong et al., Patil et al., and Danov et al. They are also probably present in the laboratory synthesis materials of Stirton et al. and Fujiwara et al. because these started with the barium salt of the carboxylic acid. When the effect of impurity divalent ions was observed on AOT and the perfluorooctanoates, it was not enough to lower the CMC significantly. However, this might not always be the case. The interaction of divalent ions with the disalt impurity would be expected to be particularly strong, and, since this would be much more surface active, this would introduce yet another complication.

It is therefore not possible to give a definitive answer on the effect of impurities on the surface behaviour of C$_n$MES and this may be a case where the Gibbs equation cannot at present be applied with any certainty as to its accuracy. Danov et al. state "finally, it should be mentioned that some authors called into question the applicability of the Gibbs equation to the case of adsorption layers from ionic surfactants...the problem can be solved by including the counterion binding in the Gibbs equation." The "some authors" are ourselves. However, while "computer purification" is now at a level where it should in principle work, it suffers from exactly the same problem as the Gibbs equation. It can only be applied when the adsorbed species are known and their bulk concentrations/activities can all be identified. The use of a surface analytical technique such as NR does improve the situation in that it determines the surface concentration of one of the components, the surfactant ion, accurately. However, for anionic surfactants the problem of *identifying* the counterion(s) remains and no amount of "computer purification" can help solve this difficulty.

Conclusions

We have devised a new laboratory synthesis of αC_nMES based on direct sulfonation of the methyl ester by SO_3 introduced from the vapour phase. From the point of view of preparing a perdeuterated sample, this is more efficient than the previous lab based synthesis of Stirton et al.[5] It is similar to the industrial synthesis, but the subsequent steps are simpler and allow a cleaner and more effective purification. A chain deuterated sample of αC_{14}MES, prepared by this means, was used to measure the surface excess directly using neutron reflection and a wide range of concentration. The adsorption isotherm could be fitted to an empirical equation close to a Langmuir isotherm. The neutron measured surface excesses were combined with the integrated Gibbs equation to fit the surface tension. The fit was exact provided that we used a prefactor consistent with the counterion at the surface being a divalent ion, as has previously been found for AOT and various perfluorooctanoates. In the presence of 100 mM NaCl this contamination was suppressed and the integrated equation could be fitted with the integrated Gibbs equation and the normal prefactor of 1. We have used our data to reinterpret measurements by Danov et al. on an unpurified sample of αC_nMES for which a computer refinement was used in an attempt to eliminate the effects of the impurities.

Acknowledgements

We thank ISIS for the provision of beam time and their technical support.

References

(1) Martnez, D.; Orozco, G.; Rincón, S.; Gil, I. Simulation and pre-feasibility analysis of the production process of α-methyl ester sulfonates. *Bioresource Technology* **2010**, *101*, 8762–8771.

(2) Maurad, Z. A.; Ghazali, R.; Siwayanan, P.; Ismail, Z.; Ahmad, A. Alpha-Sulfonated

Methyl Ester as an Active Ingredient in Palm-Based Powder Detergents. *J. Surfactants Detergents* **2006**, *9*, 161–167.

(3) Patil, S. R.; Mukaiyama, T.; Rakshita, A. K. α-Sulfonato Palmitic Acid Methyl Ester-Hexaoxyethylene Monododecyl Ether Mixed Surfactant System: Interfacial, Thermodynamic, and Performance Property Study. *J. Surfactants Detergents* **2004**, *7*, 87–96.

(4) Wong, S. P.; Lim, W. H.; Cheng, S. F.; Chuah, C. H. Properties of Sodium Methyl Ester Alpha-Sulfo Alkylate/Trimethylammonium Bromide Mixtures. *J. Surfact. Deterg.* **2012**, *15*, 601–611.

(5) Stirton, A. J.; Bistline, R. G.; Weil, J. K.; Ault, W. C.; Maurer, E. W. Sodium Salts of Alkyl Esters of α-sulfo Fatty Acids, Wetting, Lime Soap Dispersion and Related Properties. *J. Am. Chem. Oil Chem.* **1962**, *39*, 128–131.

(6) Fujiwara, M.; Okano, T.; Nakashima, T. H.; Nakamura, A. A.; Sugihara, G. A temperature study on critical micellizaUon concentration (CMC), solubility, and degree of counterion binding of -sulfonatomyristic acid methyl ester in water by electroconductivity measurements. *Colloid Polym. Sci.* **1997**, *275*, 474–479.

(7) Ohbu, K.; Fujiwara, M.; Abe, Y. Physicochemical properties of α-sulfonated fatty acid esters. *Progr. Colloid Polym. Sci.* **1998**, *109*, 85–92.

(8) Danov, K. D.; Stanimirova, R. D.; Kralchevsky, P. A.; Basheva, E. S.; Ivanova, V. I.; Petkov, J. T. Sulfonated methyl esters of fatty acids in aqueous solutions: Interfacial and micellar properties. *J. Colloid Interface Sci.* **2015**, *457*, 307–318.

(9) Xu, H.; Li, P. X.; Ma, K.; Thomas, R. K.; Penfold, J.; Lu, J. R. Limitations in the Application of the Gibbs Equation to Anionic Surfactants at the Air/Water Surface: Sodium Dodecylsulfate and Sodium Dodecylmonooxyethylenesulfate Above and Below the CMC. *Langmuir* **2013**, *29*, 9335–9351.

(10) Radke, C. J. Gibbs Adsorption Equation for Planar Fluid-Fluid Interfaces: Invariant Formalism. *Adv. Colloid Interface Sci.* **2014**, *222*, 600–614.

(11) Cross, A. W.; Jayson, G. G. The effect of small quantities of calcium on the adsorption of sodium dodecyl sulphate and calcium at the gas–liquid surface. *J. Colloid Interface Sci.* **1994**, *162*, 45–51.

(12) An, S. W.; Lu, J. R.; Thomas, R. K.; Penfold, J. Apparent anomalies in surface excesses determined from neutron reflection and the Gibbs equation in anionic surfactants with particular reference to perfluorooctanoates at the air/water interface. *Langmuir* **1996**, *12*, 2446–2453.

(13) Li, Z. X.; Lu, J. R.; Thomas, R. K. Neutron reflectivity studies of the adsorption of Aerosol-OT at the air/water interface: the surface excess. *Langmuir* **1997**, *13*, 3681–3685.

(14) Eastoe, J.; Nave, S.; Downer, A.; Paul, A.; Rankin, A.; Tribe, K. Adsorption of Ionic Surfactants at the Air-Solution Interface. *Langmuir* **2000**, *16*, 4511–4518.

(15) Weil, J. K.; Bistline, R. G.; Stirton, A. α-sulfo palmitic acid. *Organic Syntheses* **1963**, *4*, 83–86.

(16) Roberts, D. W.; Giusti, L.; Forcella, A. Chemistry of Methyl Ester Sulfonates. *Biorenewable Resources* **2008**, *5*, 2–9.

(17) Webster, J. R. P.; Langridge, S.; Dalgliesh, R. M.; Charlton, T. R. Reflectometry techniques on the Second Target Station at ISIS: Methods and science. *Eur. Physical J.Plus* **2011**, *126*, 112.

(18) Li, P. X.; Thomas, R. K.; Penfold, J. Limitations in the Use of Surface Tension and the Gibbs Equation To Determine Surface Excesses of Cationic Surfactants. *Langmuir* **2014**, *30*, 6739–6747.

(19) Fujiwara, M.; Miyake, M.; Abe, Y. Colloidal properties of α-sulfonated fatty acid methyl esters and their applicability in hard water. *Colloid Polym. Sci.* **1993**, *271*, 780–785.

(20) Downer, A.; Eastoe, J.; Pitt, A. R.; Simister, E. A.; Penfold, J. Effects of Hydrophobic Chain Structure on Adsorption of Fluorocarbon Surfactants with either CF3- or H-CF2-Terminal Groups. *Langmuir* **1999**, *15*, 7591–7599.

(21) Zimmerman, J.; Banks, C. V. Some properties of sulfoacetic acid and 3-sulfopropionic acid and their use as analytical masking agents. *Ames Laboratory ISC Technical Reports* **1956**, *147*.

(22) Maurad, Z. A.; Ghazali, R.; Siwayanan, P.; Ismail, Z.; Ahmad, S. Alpha-Sulfonated Methyl Ester as an Active Ingredient in Palm-Based Powder Detergents. *J. Surfactants Detergents* **2006**, *9*, 161–166.

(23) Xie, T. .; Zeng, C. F.; Wang, C. Q.; Zhang, L. X. Preparation of Methyl Ester Sulfonates Based on Sulfonation in a Falling Film Microreactor from Hydrogenated Palm Oil Methyl Esters with Gaseous SO_3. *Ind. Eng. Chem. Res.* **2013**, *52*, 3714–3722.

(24) Yamada, K.; Matsutani, S. Analysis of the Dark-Colored Impurities in Sulfonated Fatty Acid Methyl Ester. *J. Am. Oil Chem. Soc* **1996**, *73*, 121–125.

(25) Carpena, P.; Aguiar, J.; Bernaola-Galvan, P.; Carnero Ruiz, C. Problems Associated with the Treatment of Conductivity-Concentration Data in Surfactant Solutions: Simulations and Experiments. *Langmuir* **2002**, *18*, 6054–6058.

(26) Sugihara, G.; Nakamura, A. A.; Nakashima, T. H.; Araki, Y. I.; Okano, T.; Fujiwara, M. An ElectroconducUvity Study on Degree of Counterion Binding or Dissociation of α–sulfonatomyristic Acid Methyl Ester Micelles in Water as a Function of Temperature. *Colloid Polym Sci.* **1997**, *275*, 790–796.

(27) Mysels, K. J.; Otter, R. J. Conductivity of Mixed Sodium Decyl and Dodecyl Sulfates–the Composition of Mixed Micelles. *J. Colloid Interface Sci.* **1961**, *16*, 462–473.

(28) Tokiwa, F.; Moroyima, N. Mixed Micelle Formation of Anionic and Nonionic Surfactants. *J. Colloid Interface Sci.* **1969**, *30*, 338–344.

(29) Weil, J. K.; Stirton, A. Critical Micelle Concentrations of α–sulfonated fatty acids and their esters. *J. Am. Chem. Soc.* **1956**, *60*, 899–901.

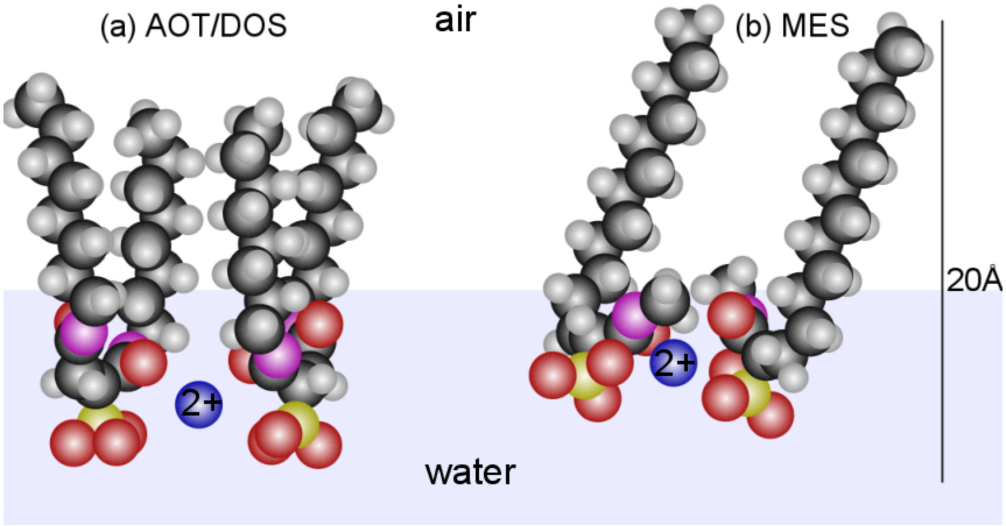

Figure 8: TOCGraphic